



Published in final edited form as:

Ann Biomed Eng. 2017 January ; 45(1): 23–44. doi:10.1007/s10439-016-1678-3.

3D Printing of Calcium Phosphate Ceramics for Bone Tissue Engineering and Drug Delivery

Ryan Trombetta^{1,2}, Jason A. Inzana^{2,4}, Edward M. Schwarz^{1,2,3}, Stephen L. Kates^{2,5}, and Hani A. Awad^{1,2,3}

¹Department of Biomedical Engineering, University of Rochester, Robert B. Goergen Hall, Rochester, NY 14627, USA ²Center for Musculoskeletal Research, University of Rochester Medical Center, 601 Elmwood Avenue, Box 665, Rochester, NY 14642, USA ³Department of Orthopedics, University of Rochester Medical Center, 601 Elmwood Avenue, Rochester, NY 14642, USA ⁴AO Research Institute Davos, Clavadelerstrasse 8, 7270 Davos, Switzerland ⁵Department of Orthopaedic Surgery, Virginia Commonwealth University School of Medicine, Richmond, VA 23298, USA

Abstract

Additive manufacturing, also known as 3D printing, has emerged over the past 3 decades as a disruptive technology for rapid prototyping and manufacturing. Vat polymerization, powder bed fusion, material extrusion, and binder jetting are distinct technologies of additive manufacturing, which have been used in a wide variety of fields, including biomedical research and tissue engineering. The ability to print biocompatible, patient-specific geometries with controlled macro- and micropores, and to incorporate cells, drugs and proteins has made 3D-printing ideal for orthopaedic applications, such as bone grafting. Herein, we performed a systematic review examining the fabrication of calcium phosphate (CaP) ceramics by 3D printing, their biocompatibility *in vitro*, and their bone regenerative potential *in vivo*, as well as their use in localized delivery of bioactive molecules or cells. Understanding the advantages and limitations of the different 3D printing approaches, CaP materials, and bioactive additives through critical evaluation of *in vitro* and *in vivo* evidence of efficacy is essential for developing new classes of bone graft substitutes that can perform as well as autografts and allografts or even surpass the performance of these clinical standards.

Keywords

3D printing; Vat polymerization; Powder bed fusion; Material extrusion; Binder jetting; Bone; Tissue engineering; Drug delivery

INTRODUCTION

Three-dimensional (3D) printing, also known as additive manufacturing, is a digital fabrication process in which geometrical data are used to produce 3D solids by incremental addition of material layers. Charles Hull pioneered the modern idea of 3D printing when he first described a vat polymerization method, known as stereolithography (SL), in a 1984 patent.⁴¹ The advent of this new photopolymer-based fabrication technique ushered in the era of rapid and economical production of physical prototypes directly from computer-aided designs, with near limitless geometrical complexity. Originally focused on rapid prototyping of preliminary concept models, advances in materials and technologies are enabling the creation of functional products; and thus, are transitioning these fabrication techniques from prototyping to mainstream manufacturing applications. Beyond vat polymerization, other additive technologies including powder bed fusion, material extrusion, and binder jetting,³ have since been developed, and are discussed in more detail in the following sections.

3D printing is being adopted in nearly every industry, including the medical field, with extensive research pursuits focused on novel materials and combinations of techniques that could enhance product functionality and reduce costs. For example, 3D printing an object can enable formation of composites with controlled spatial heterogeneity for superior structure–function relationships that are unachievable with traditional strategies such as machining. This vast potential has made 3D printing extremely popular in the fields of biomedical research and tissue engineering, due to the ability to replicate the intricate architecture as well as the cellular and constituent heterogeneity of tissues and organs.⁶⁷ Bone, for example, is a complex composite of minerals (mostly calcium phosphates (CaP)) and organic matrix (mostly type I collagen) with exquisite structural organization. This organization spans multiple size scales, such as cortical vs. trabecular bone at the macro-scale and lamellar osteons at the micro-scale. The organization of bone can in theory be imitated using 3D printing. Additionally, 3D printing is amenable to producing patient-specific geometries that are derived from medical images, such as CT scans. This paper systematically reviews progress in 3D printing strategies over the past decade, which have been utilized for bone repair and tissue engineering, with a specific focus on 3D printed pure or composite CaP ceramic scaffolds. The review contrasts the advantages and disadvantages of low-temperature printing vs. high-temperature postprocessing for bone tissue engineering applications. It also reviews the state-of-the-art in 3D printed scaffolds for cell and drug delivery *in vitro* and *in vivo* in applications involving bone repair and regeneration as well as management of infection.

THREE-DIMENSIONAL PRINTING PROCESSES

Vat Polymerization

In the vat polymerization process (e.g., stereolithography), a photo-curable liquid polymer is selectively polymerized at the surface of a vat by a low-power ultraviolet (UV) light source. As the z-axis is translated down, a new thin layer of liquid is spread over the solid surface and this process is repeated until the build is complete (Fig. 1a). Continuous liquid interface production (CLIP) 3D printing has recently been described as an innovative vat polymerization technique that uses UV laser for photocuring and oxygen to create a non-

polymerized dead zone to enable the projection of continuous solid objects without the lamination typically seen in standard layer by layer SLA polymerization.⁸⁴ Some polymers that have been used with vat polymerization for bone tissue engineering applications include poly(propylene fumarate) (PPF)⁵⁷ and poly(ϵ -caprolactone fumarate) (PCLF)⁹⁰ as well as PPF/PCLF blends⁸⁷ (Table 1). Supplementing these polymers with hydroxyapatite (HA) nanoparticles has been shown to increase the elastic modulus and potentially enhance the osteoconductivity^{55,58,88} Alternatively, vat polymerization has also been employed to produce complex sacrificial molds for HA scaffolds, which are pyrolyzed before or during sintering of the ceramic.¹⁸ The primary advantages of vat polymerization are: (1) the fine resolution that enables interconnected pore diameters and wall thicknesses as small as 100 μm , (2) the tunability of the scaffold stiffness due to the variety of polymers that can be printed and the degree to which crosslinking can be controlled, and (3) the potential for incorporation of bioactive molecules within the polymer.^{51,56} For bone tissue engineering, vat polymerization is constrained to photo-curable polymers and can be limited in terms of the amounts of ceramic additives.

Powder Bed Fusion

Powder bed fusion (e.g., laser sintering) employs a fine resolution laser or electron beam to achieve selective thermal binding of materials in a layer-by-layer fashion, but unlike liquid photopolymers used in vat polymerization, solid particles from a variety of materials can be bound together by partial or full melting (Fig. 1b). New thin layers of powder are then rolled out over the previous layer and the process is repeated until the build is complete. Materials that have been utilized with these fabrication methods for bone applications include plastics such as poly(ϵ -caprolactone) (PCL),⁹³ biphasic calcium phosphates,⁷⁶ polymer/calcium phosphate composites,^{24,60,95} and titanium alloys⁸⁵ (Table 1). Although these materials are generally viewed as osteoconductive, they are unable to facilitate complete bone healing without the addition of cells or growth factors. In one study, bone regeneration was enhanced in a rat segmental femoral defect by augmentation of porous titanium scaffolds with growth factor-laden gelatin hydrogels after printing.⁸⁶ The primary advantage of powder bed fusion is the production of highly detailed, high strength porous scaffolds, which could be used in partial or full load-bearing applications, as in the case of titanium. However, sintering of plastics, ceramics and metals produces localized ultra high temperatures, which preclude the potential for simultaneous incorporation of cells, proteins, or heat-labile bioactive molecules.

Material Extrusion

Material extrusion encompasses any process in which materials are deposited as continuous strands through a nozzle or a dispensing orifice in an incremental layer-by-layer fashion that will yield a 3D product upon solidification of the extruded material (Fig. 1c). A wide variety of material extrusion techniques have been devised and are referred to by an expanding terminology including, but not limited to, 3D (bio)plotting, dispense plotting, or bioprinting which can be used to print bioadditive- and cell-laden hydrogels, to be cross-linked once extruded. In addition extrusion can be achieved by dispensing nearly molten plastic filament through a nozzle (e.g., thermal material extrusion). The material then cools and solidifies into the final 3D form. Material extrusion techniques are the most widely employed 3D

printing strategies for tissue engineering, which have led to remarkable progress in the field. This technology has been recently advanced to enable multi-material printing that include cell-laden hydrogels, supporting polymer fibers and sacrificial materials, and has demonstrated the ability to fabricate human-scale tissues of any form including mandible, calvarial bone, cartilage and skeletal muscle.⁴⁸

With specific focus on bone applications, extrusion-based systems have employed the widest variety of materials using multiple deposition techniques. These materials include synthetic polymers such as polyesters,^{54,74,75,77} natural polymers such as alginate,^{69,70} and polymer/ceramic (including bioactive glass) composites^{30,47,50,54,59,62,73,94,97} (Table 1). While ceramics that are printed by material extrusion often require a secondary heat treatment or sintering, some polymer-based or hybrid scaffolds can be fabricated under mild conditions that are amenable to simultaneous incorporation of growth factors or live cells.^{69,70,75} The resolution of these techniques depends on the diameter of the dispensing nozzles and the stability of the material after extrusion. Extruded strands commonly have a diameter of 100–200 microns. In some cases, which may depend on the material or geometry, an additional sacrificial support material might be necessary for the scaffolds to maintain form until they can be post-processed.

Binder Jetting

Similar to powder bed fusion, binder jetting selectively binds particulate materials in a layer-by-layer fashion. Instead of fusing the particles with lasers or an electron beam, binder jetting selectively sprays one or more binding solutions from inkjets to unify the particles (Fig. 1d). In bone tissue engineering, the powder phase is most often a CaP, such as tricalcium phosphate (TCP) or hydroxyapatite (HA) (Table 1). The binding solution is usually a sacrificial polymer, which is pyrolyzed during sintering after printing, or an aqueous solution. CaP powders typically require aqueous binding solutions, such as dilute phosphoric acid (in a concentration range of 5–30 wt.%). The acidic binder initiates a dissolution-precipitation reaction within the powder to fuse the particles.³⁵ Typically, a commercial 3D inkjet printer is minimally adapted for printing CaP bone graft substitutes. These printers utilize thermal or piezoelectric inkjet cartridges that are identical to those found in common desktop printers. These ink cartridges can be opened, cleaned, and refilled with the binder solution or bioactive ‘inks’.

The solubility of CaP in the aqueous binder is an important parameter of printability and it depends on its mineral phase as summarized in Table 1. It should be noted that the solubility properties of a given CaP phase can vary depending on synthesis techniques and environmental conditions.^{25,33} The approximate solubility product constants (K_{sp}) provided in Table 2 indicate equilibrium solubility conditions in a specific chemical system, which is independent of pH and does not represent the absolute dissolution. Solubility isotherms as a function of pH can be better indicators of dissolution and such calculations have been performed for all of the CaP phases listed in Table 1.^{9,46} Furthermore, mixing CaP with more reactive minerals such as calcium sulfates (CS) has also been shown to improve solubility and binding using aqueous binders, independent of pH.^{82,99}

A comprehensive review of CaP for bone regeneration using fabrication techniques other than 3D printing is beyond the scope of this review, but the interested reader is referred to previous reviews of the topic.^{6,8,10,16,17} The CaP phase most commonly used in binder jetting is α -TCP, which is more thermodynamically unstable (and thus more soluble) than β -TCP.¹¹ When TCP is combined with phosphoric acid, the dissolution-precipitation reaction yields brushite ($\text{CaHPO}_4 \cdot 2\text{H}_2\text{O}$). Butscher and colleagues demonstrated the superior binder jetting quality and geometrical accuracy of α -TCP vs. β -TCP when using 10% phosphoric acid as the binder solution.¹² This study also examined the effects of particle size on printability and observed that when the particle size is too small, flowability is compromised due to agglomeration of the particles, resulting in surface mottling of the powder bed. If the particle size is too large, the powder flows easily but does not pack sufficiently, causing interlayer instability that compromises binding and geometrical accuracy. Powder particles in the size range of 10–50 microns are generally considered optimal.^{12,43,52,99}

SYSTEMATIC REVIEW OF THE LITERATURE: SEARCH ALGORITHM AND INCLUSION/EXCLUSION CRITERIA

The PubMed database was searched on January 5th, 2016 using the string '(3D printing OR 3D printed OR rapid prototyping OR additive manufacturing OR inkjet OR granular material binding) AND (bone OR scaffold OR graft) AND (bioceramic OR ceramic OR calcium phosphate)' to identify articles that investigated the use of 3D-printing to fabricate CaP scaffolds for bone graft substitutes. The search was limited to publications within the last 10 years. Articles in languages other than English were excluded and all reviews were omitted. This search returned 103 results. Studies that utilized 3D-printing, but did not directly involve calcium phosphate in the printing process or bone applications were excluded, as were papers that focused only on optimization or characterization of chemical or mechanical properties of 3D-printed CaP scaffolds with no biological or *in vivo* assessments. Additional studies that were not returned in the PubMed search, but were identified to be relevant to the topic of this review were included. With this search algorithm and inclusion/exclusion criteria, a total of 45 articles involving *in vitro* and *vivo* approaches for bone tissue engineering or drug delivery were fully reviewed and discussed herein, as summarized in Tables 3, 4, 5, 6, and 7. The reviewed papers were broadly categorized into bone regeneration and drug delivery studies in the context of bone repair and infection, which were then further classified into low- and high-temperature 3D printing approaches.

3D PRINTING FOR BONE REGENERATION

Low Temperature 3D Printing of CaP Scaffolds for Bone Regeneration

Of the papers reviewed in Table 3, the majority used binder jetting approaches, and two studies investigated material extrusion approaches. As described earlier, acidic binder solutions applied to CaP powders in binder jetting enable low temperature binding of the particles in a dissolution-precipitation reaction. In material extrusion, CaP slurries or cements are typically extruded through a non-heated print-head or nozzle under mild conditions, and the extruded materials are then solidified in a variety of ways based on their chemical composition. For example, extruded CaP (composed primarily of α -TCP) paste in

a carrier liquid composed of short-chain triglyceride are solidified by placement in water to initiate the cement-setting reaction in just a few minutes, and can be further hardened by incubation at 37 °C for several hours.⁶¹ Photocurable hydrogels (poly(ethylene glycol)dimethacrylate (PEGDMA)) with suspended MSCs, bioactive glass (BG), and hydroxyapatite (HA) particles are photo polymerized by UV light.³² Poly(lactic acid) (PLA) (with 5% PEG) polymer blend with BG are cross-linked with NaOH (8% w/v) in 70% ethanol deposited during the 3D printing process and then set by evaporation of the solvent chloroform.²

Regardless of the fabrication method or material, for regenerative applications it is necessary to determine the biocompatibility of the 3D printed scaffold. This is commonly accomplished by seeding cells onto the scaffold and assessing cell viability and proliferation, among a variety of other biological responses.^{15,32,43,61} Indeed, seeded cells have been shown to attach to a variety of 3D printed scaffolds and achieve a normal cell morphology.^{43,61,79} In binder jetting, additives to either the binder solution or CaP powder have been shown to affect cell behavior.^{15,43} For example, Inzana *et al.* (2014) added solubilized collagen to a phosphoric acid binder solution and observed a significant improvement in relative cell viability (normalized to tissue culture plastic) of C3H/10T1/2 cells seeded onto CaP scaffolds.⁴³ Additionally, Castilho *et al.* (2015) demonstrated that mixing CaP powder with alginate, enhanced both cell viability and cell proliferation, while vacuum infiltration of alginate into the printed scaffold reduced both cell viability and cell proliferation of the osteoblastic cell line MG63.¹⁵ For material extrusion, Lode *et al.* (2014) showed that human mesenchymal stem cells (hMSCs) attached to a CaP cement scaffold, and the attachment was improved by inducing osteogenic differentiation of hMSCs prior to seeding.⁶¹

Low temperature extrusion 3D printing of CaP scaffolds enables direct printing of living cells suspended in 'bioinks'.³² Investigating the composition of a variety of bioinks consisting of poly(ethylene glycol) dimethacrylate (PEGDMA), BG, HA, and hMSCs Gao *et al.* (2014) found that cell viability of directly printed hMSCs was highest in pure PEGDMA and PEGDMA-HA bioinks, while PEGDMA-BG had a significantly lower cell viability. The presence of HA in the bioink also led to differentiation towards the osteoblastic lineage. The high resolution (ink drops <0.03 mm diameter) achieved by this material extrusion approach enables precise patterning of cells within the CaP scaffold, which overcomes limitations of post-printing seeding of cells, including reduced cell attachment and inhomogeneous cellular distribution within the porous scaffolds. Mehrban *et al.* (2013) showed that preconditioning 3D printed CaP scaffolds in acellular and cellular *in vitro* conditions can help obtain desired physical characteristics for *in vivo* implementation.⁶⁵ Morphological changes of 3D printed CaP scaffolds occurred when immersed in culture media over a 28-day period. These changes included an increase in porosity and fluctuations in surface roughness suggesting degradation of the exterior layer of the CaP scaffold. However, the seeding of cells (tenocytes) and the production of ECM on the CaP scaffolds inhibited dissolution and morphological changes.⁶⁵ Thus, it is important to recognize that not only does the scaffold affect cell function, but the seeded cells can also play an important role in stabilizing the scaffold and controlling its degradation.

When implanted *in vivo*, scaffolds can elicit a host inflammatory response, but it is not fully understood how this might affect regeneration since inflammation is an important stage in bone repair.^{38,66,96} Almeida *et al.* (2014) demonstrated that the immune response of macrophages to 3D printed CaP scaffolds *in vitro* is sensitive not only to surface properties (i.e., surface chemistry) but also to scaffold geometry (porosity and pore size).² More research is needed to determine the ideal response and cytokine environment for favorable scaffold-initiated bone regeneration.

3D printed CaP bone graft substitutes fabricated at low temperatures have been shown to be osteoconductive *in vivo* in a variety of orthotopic implantation models.^{39,42,43,53} Inzana *et al.* (2014) showed that binder jetting (inkjet) 3D printed CaP scaffolds with and without incorporated collagen stimulated bone ingrowth and served as osteoconductive spacers in a critically sized murine femoral defect.⁴³ However, CaP-collagen composites did not improve *in vivo* bone regeneration and complete bridging of the defect. The osteoconductivity of the binder jetting 3D printed TCP scaffolds has been shown to be better than that of HA scaffolds.⁴² Interestingly, while the size of macropores in 3D printed CaP scaffolds has been shown to affect osteoconductivity and bone regeneration *in vivo*,⁴² Habibovic *et al.* (2008) reported that pore morphology (open vs. closed macropores of comparable size of 1.3 mm) had no effect on new bone formation in a goat decorticated lumbar implant.³⁹

High Temperature 3D Printing of CaP Scaffolds for Bone Regeneration

The production of CaP scaffolds at high temperatures is necessary for certain 3D printing techniques (i.e., powder bed fusion or thermal material extrusion). Moreover, high temperature post-processing techniques (i.e., heat sintering) applied to 3D printed CaP scaffolds have the primary benefit of enhancing mechanical strength. However, these high temperature limit the ability to incorporate heat-labile biofactors or cells during the fabrication process. This section examines 3D printed CaP scaffolds fabricated or postprocessed at high temperatures without incorporated drugs or growth factors. The studies reviewed in Tables 4 and 5 mostly used material extrusion or binder jetting to fabricate pure or composite CaP scaffolds, and assessed their osteogenic potential *in vitro* or *in vivo*, and far fewer studies used powder bed fusion or vat polymerization.

CaP scaffolds printed at high temperatures were characterized *in vitro* to assess biocompatibility (Table 4). A wide variety of cells have been used for such characterization, including osteoblasts,^{7,14,20,24,71,91} preosteoblastic cells,^{19,49} stromal cells,^{22,71,98} osteoclasts,²¹ mesenchymal stem cells (MSCs),^{68,72} epithelial cells,⁴ and Schwann cells.⁸⁰ Cell viability,^{14,21,22,24,71,80,98} proliferation,^{14,19,21,22,24,32,40,68,71,72,80,91} and cytotoxicity^{19,91} assays all show a general consensus of favorable biocompatibility regardless of the 3D printing method using different biomaterials. Furthermore differentiation of MSCs seeded on 3D printed CaP scaffolds into the osteoblastic lineage was only evident when culturing with osteogenic media^{21,68,71} or an osteoinductive element (e.g., mesoporous glass⁹⁸). Yet one study demonstrated the ability of HA/TCP scaffolds fabricated by vat polymerization to induce seeded MSCs to differentiate into osteoblast-like cells without osteogenic media as determined by expression of osteogenic markers *in vitro* and improved calvaria defect repair *in vivo*.⁷² Cells not directly involved in the production

or resorption of bone have also been seeded and characterized on 3D printed CaP scaffolds to indirectly enhance bone regeneration by supporting innervation and angiogenesis. Sweet *et al.* (2015) demonstrated that extruding patterned β -TCP composite scaffolds can support the growth of viable Schwann (SC) cells and develop normal nerve-related cell phenotypes and morphologies.⁸⁰

Castilho *et al.* (2014) investigated how the composition of CaP (Ca/P ratio) affects biocompatibility, and concluded that biphasic TCP and HA scaffolds produced by binder jetting¹⁴ enhanced seeded osteoblasts' cellular response (viability and proliferation), compared to pure TCP scaffolds. However, Seol *et al.* (2014) reported that 3D printed HA scaffolds produced from a slurry mixture of ceramic powder with photocurable resin (FA1260T; a urethane acrylate monomer) by vat polymerization, and suggested that these scaffolds promote proliferation of osteoblasts and MSCs, while HA-TCP scaffolds fabricated similarly promote osteoblastic differentiation *in vitro*.

Almost half of the studies utilizing high temperature 3D printing of CaP scaffolds investigated bone regeneration *in vivo* (Table 5). The enhanced mechanical properties of CaP scaffolds produced at high temperatures enable them to be structurally sound when orthotopically implanted, especially in load bearing models. Results of these studies showed varying degrees of osteoconductivity for 3D printed CaP scaffolds and collectively conclude that 3D printed CaP scaffolds alone generally do not stimulate bone healing and regeneration compared to autologous bone grafts.⁸¹

Osteoinductive dopants or surface modifications were often incorporated pre- or post-fabrication to better enhance the bone regenerative potential of 3D printed CaP scaffolds. Doping 3D printed CaP scaffolds with metal oxides or incorporating additional bioactive materials have been shown to enhance osteoinductivity.^{29,98} For example, doping raw CaP powder with both SiO₂ and ZnO, prior to 3D printing (binder jetting) of CaP scaffolds and post-fabrication sintering at 1250 °C, have been reported to enhance both osteogenic differentiation, as well as neovascularization in a load-bearing rat femoral defect reconstructed with the printed scaffolds.²⁹ CaP scaffolds prepared by material extrusion of β -TCP-PVA slurry and subsequently surface coated with a nanolayer of mesoporous BG and annealed at 650 °C enhanced bone regeneration and angiogenesis in a rabbit calvaria defect model compared to non-coated β -TCP-PVA scaffolds.⁹⁸ Wang *et al.* (2014) performed unique post-fabrication modifications to extruded CaP scaffolds, by creating a “virus activated matrix or VAM” wherein RGD-phage nanofibers act as a mimetic ECM for enhanced attachment of endothelial and osteo-progenitor cells, and demonstrated that this approach leads to enhanced vascularization and bone regeneration in a load bearing rat radius defect.⁸⁹

Cell seeding on 3D printed scaffolds has also been investigated as a strategy for enhancing bone regenerative potential *in vivo*. For example, Barboni *et al.* (2013) demonstrated the osteogenic potential of ovine amniotic epithelial cells (oAEC) seeded on a CaP scaffold fabricated by material extrusion of a paste-like aqueous ceramic slurry of HA/ β -TCP.⁴ When implanted in sheep to augment maxillary sinus defects, oAEC-seeding of the 3D printed CaP

scaffolds significantly increased bone ingrowth into the defect and accelerated angiogenesis when compared to scaffolds without cells.

3D PRINTING FOR DRUG DELIVERY

Low Temperature 3D Printing of CaP Scaffolds for Drug and Growth Factor Delivery

CaP scaffolds produced by binder jetting at low temperature ($<37^{\circ}\text{C}$) are theoretically amenable to incorporation of heat-labile bioactive molecules for localized and controlled delivery. These molecules include growth factors to promote angiogenesis and bone regeneration or antibiotics to combat bone infections (Table 6). While it is possible to adsorb growth factors and drugs onto the 3D printed CaP scaffolds after post-processing,^{5,36,37} the amount of drug adsorption and kinetics of release vary depending on the CaP phase used and the method of drug loading. Regardless, this approach results in burst release of the surface-adsorbed drug within hours and almost consistently fails to sustain release beyond 24 h *in vitro*. The potential to enable homogeneous volumetric drug loading and to create spatial gradients or site-specific drug localization within a scaffold using 3D printing may offer significant functional advantages over surface adsorption and could dramatically enhance the therapeutic potential of these 3D printed scaffolds. Yet, few studies investigated this approach using low temperature 3D printing and pure CaP scaffolds. In a study by Inzana *et al.* (2015), volumetric incorporation of antibiotics within 3D printed CaP scaffolds was evaluated as a treatment strategy for implant associated bone infection (osteomyelitis). Cylindrical CaP scaffolds produced by binder jetting incorporated antibiotics either by mixing vancomycin and rifampin directly with phase-pure α -TCP or direct jetting as “bioink” from the color inkjets along with the phosphoric acid binder from the black inkjet cartridge.⁴⁴ Strategies to control the release kinetics by post-printing coating of the CaP scaffolds with poly (D,L-lactide-*co*-glycolide) (PLGA) achieved first-order release kinetics, sustained the release over 14 days *in vitro* and *in vivo*, and improved flexural biomechanics to values reaching those of dense cancellous bone.⁴⁴ Interestingly, these CaP scaffolds with incorporated antibiotics significantly reduced the bacterial burden in a mouse model of established femoral osteomyelitis.⁴⁴

Material extrusion can be more versatile than binder jetting, and when performed under low temperature and mild post-processing conditions it can be amenable to generating drug- or growth factor-loaded composite CaP scaffolds. Mineralized slurry or paste compositions, which can be extruded at physiologic temperature are especially suited for this approach. Martínez-Vázquez *et al.* (2015) demonstrated the feasibility of 3D printing of porous silicon-doped hydroxyapatite and gelatin (HASi/G) composite scaffolds for delivery of vancomycin.⁶⁴ These scaffolds behaved as hydrogels, but displayed compressive strength-mineral density relationships that were closer to cancellous than cortical bone, and in general showed a favorable biocompatibility profile *in vitro*. When loaded with vancomycin, the HASi/G scaffolds achieved first-order diffusive release kinetics, but did not sustain release beyond 10 h *in vitro*. Furthermore, the incorporation of the antibiotic under the mild scaffold fabrication conditions maintained the drug’s antimicrobial activity in standard *in vitro* assays.⁶⁴ Akkineniet *al.* (2015) described a similar approach of extruding α -TCP-based CaP cement (CPC) premixed with chitosan/dextran sulphate microparticles encapsulating

vascular endothelial growth factor (VEGF) or bovine serum albumin (BSA) in a liquid carrier consisting of a biocompatible oil.¹ The extruded CPC scaffolds had compressive strength and moduli in the range of the compressive properties of trabecular bone. The biocompatibility of the scaffolds was demonstrated by the viability and alkaline phosphatase activity of mesenchymal stem cells cultivated on the scaffolds for up to 21 days.

While extrusion of CaP composite pastes and hydrogels has the advantage of permitting premixing with drugs and growth factors, this usually means lower printing resolution due to viscosity of these flowable mineralized slurries, which requires large nozzle diameters (>500 microns). The liquid carriers can be organic hydrogels or inorganic carriers, and both require post-processing to allow them to set and harden. Few studies have investigated the performance of 3D printed CaP composites *in vivo*. Poldervaart *et al.* (2013) used material extrusion to fabricate composite macroporous alginate scaffolds, which were laden with gelatin microparticles (GMPs) and mesenchymal stem cells.⁷⁰ The resulting scaffolds had a uniformly distributed array of pores on the order of 500 microns with alginate struts as wide as 2 mm. Due to the viscosity of the composite alginate suspension, concentrations greater than 3% w/v alginate could not be extruded, and this seemed to affect the stability of the printed scaffolds. While this study demonstrates the feasibility of bioprinting CaP composites, and provides one of few examples of *in vivo* proof of concept, it also highlights the limitations of extrusion based bioprinting; namely the low resolution and the effects of the flowable polymer viscosity on printability.

High Temperature 3D Printing of CaP Scaffolds for Drug and Growth Factor Delivery

High temperature fabrication methods or high temperature post-processing techniques have the primary benefit of enabling CaP ceramics to achieve enhanced mechanical properties. Yet, this methodology hinders the ability to uniformly print cells and/or bioactive molecules. To circumvent this limitation, additional post-processing techniques can be utilized to incorporate biofactors and cells onto the printed construct including surface adsorption or surface modifications, irrespective of the 3D printing technology (Table 7). The most common additive is BMP-2, which is typically incorporated during the post-processing steps to add an osteoinductive element. For example, Duan *et al.* (2010) utilized a modified commercial laser sintering (powder bed fusion) system to fabricate composite scaffolds from CaP/poly(hydroxybutyrate-co-hydroxyvalerate) (PHBV) microspheres.²³ Rectangular scaffolds with designed macropores of 2 mm evenly patterned throughout the scaffold were fabricated with layer thickness (resolution) of 0.1 mm. This study demonstrated the favorable *in vitro* biocompatibility of the laser-sintered CaP scaffolds with heparin surface modifications and BMP-2 adsorption, but lacked characterization of drug release kinetics.

El-Ghannam *et al.* (2013) adsorbed rhBMP-2 onto sintered silicon doped CaP (SCaP) scaffolds produced by binder jetting and then implanted these scaffolds into a 10 mm rabbit ulna defect.²⁷ Silicon doped CaP has been shown to enhance both the bioactivity and mechanical properties of CaP scaffolds and in combination with rhBMP-2 these CaP scaffolds enabled bone ingrowth, osseointegration, and vascularization.^{27,28} Strobel *et al.* (2014) fabricated CaP scaffolds composed of HA, β -TCP, and of an acid-hydrolytic modified

potato starch (dextrin) powder using a commercial inkjet 3D-printer with water-glycerol as a binder solution.⁷⁸ When coated with fibrin premixed with BMP-2 or seeded with osteoblasts, and implanted in subcutaneous pockets in rats, significant ectopic bone formation was observed. One study demonstrated that osteoinductive elements, other than BMP-2 or cells, can be incorporated into 3D-printed CaP scaffolds for enhancing bone formation. Ishack *et al.* (2015) extruded biphasic CaP (15% HA and 85% β -TCP) in a colloidal gel ink, and then loaded these scaffolds with either BMP-2 or dipyridamole, a drug that upregulates extracellular adenosine.⁴⁵ When implanted into a mouse calvarial defect, both BMP-2 and dipyridamole loaded scaffolds promoted bone regeneration 8 weeks post-operatively.

CONCLUSIONS

In summary, CaP scaffolds produced using approaches involving low- or high-temperature 3D printing processes or post-processing steps have been shown to be osteoconductive in a variety of animal models; however, complete bone regeneration is typically not achieved without the addition of osteoinductive elements such as cells or biofactors. Future work must focus on refining the right combination of cell populations, growth factors, or other osteoinductive elements needed for complete bone regeneration in orthotopic models of bone regeneration. It is also not known precisely what porosity and pore size distribution are ideal for supporting and enabling bone growth, but this information is vital for optimizing sintering temperatures and duration that affect both mechanical strength and pore morphologies. The advantages of low temperature fabrication approaches are nullified by the poor biomechanical properties of these scaffolds, which makes their use in load-bearing orthotopic models of bone repair challenging. New binders or printing technologies that could improve the mechanical properties of printed CaP scaffolds at biologically-relevant temperatures are an area of research that requires attention. The current 3D printing platforms have limitations intrinsic to the technology used, as described, and future research and development should focus on overcoming these limitations with the goals of enhancing biomechanical properties, resolution, biocompatibility, and sustained drug release that could approach first- or zero-order kinetics. However, an argument can be made that the 3D printing technology has matured to the point where further testing in large animals is required to demonstrate level I preclinical evidence of efficacy.

Acknowledgments

This research was supported by grants from the AO Trauma Research Institute - Clinical Priority Program on Bone Infection and the National Institutes of Health (NIH P30 AR061307 and R34 DE025573). Jason Inzana was supported in part by a Whitaker International Program post-doctoral scholarship and a National Science Foundation graduate research fellowship (NSF Award DGE-1419118). The content is solely the responsibility of the authors and does not necessarily represent the official views of AO Trauma, NIH, NSF, or the Whitaker International Program.

References

1. Akkineni AR, Luo Y, Schumacher M, Nies B, Lode A, Gelinsky M. 3D plotting of growth factor loaded calcium phosphate cement scaffolds. *Acta Biomater.* 2015; 27:264–274. [PubMed: 26318366]

2. Almeida CR, Serra T, Oliveira MI, Planell JA, Barbosa MA, Navarro M. Impact of 3-D printed PLA-and chitosan-based scaffolds on human monocyte/macrophage responses: unraveling the effect of 3-D structures on inflammation. *Acta Biomater.* 2014; 10:613–622. [PubMed: 24211731]
3. ASTM F2792-12a, Standard Terminology for Additive Manufacturing Technologies. West Conshohocken, PA: 2012. <http://www.astm.org/>
4. Barboni B, Mangano C, Valbonetti L, Marruchella G, Berardinelli P, Martelli A, Muttini A, Mauro A, Bedini R, Turriani M, Pecci R, Nardinocchi D, Zizzari VL, Tete S, Piattelli A, Mattioli M. Synthetic bone substitute engineered with amniotic epithelial cells enhances bone regeneration after maxillary sinus augmentation. *PLoS One.* 2013; 8:e63256.doi: 10.1371/journal.pone.0063256 [PubMed: 23696804]
5. Barralet J, Gbureck U, Habibovic P, Vorndran E, Gerard C, Doillon CJ. Angiogenesis in calcium phosphate scaffolds by inorganic copper ion release. *Tissue Eng A.* 2009; 15:1601–1609. DOI: 10.1089/ten.tea.2007.0370
6. Barrere F, van Blitterswijk CA, de Groot K. Bone regeneration: molecular and cellular interactions with calcium phosphate ceramics. *Int J Nanomed.* 2006; 1:317–332.
7. Bergemann C, Cornelsen M, Quade A, Laube T, Schnabelrauch M, Rebl H, Weissmann V, Seitz H, Nebe B. Continuous cellularization of calcium phosphate hybrid scaffolds induced by plasma polymer activation. *Mater Sci Eng C Mater Biol Appl.* 2016; 59:514–523. DOI: 10.1016/j.msec.2015.1010.1048 [PubMed: 26652403]
8. Black, J.; Hastings, G. *Handbook of Biomaterial Properties.* New York: Springer; 1998.
9. Bohner M. New hydraulic cements based on alpha-tricalcium phosphate-calcium sulfate dihydrate mixtures. *Biomaterials.* 2004; 25:741–749. [PubMed: 14607514]
10. Bose S, Tarafder S. Calcium phosphate ceramic systems in growth factor and drug delivery for bone tissue engineering: a review. *Acta Biomater.* 2011; 8(4):1401–1421. [PubMed: 22127225]
11. Brunner TJ, Grass RN, Bohner M, Stark WJ. Effect of particle size, crystal phase and crystallinity on the reactivity of tricalcium phosphate cements for bone reconstruction. *J Mater Chem.* 2007; 17:4072.
12. Butscher A, Bohner M, Roth C, Ernstberger A, Heuberger R, Doebelin N, von Rohr PR, Muller R. Printability of calcium phosphate powders for three-dimensional printing of tissue engineering scaffolds. *Acta Biomater.* 2012; 8:373–385. [PubMed: 21925623]
13. Castilho M, Dias M, Vorndran E, Gbureck U, Fernandes P, Pires I, Gouveia B, Armes H, Pires E, Rodrigues J. Application of a 3D printed customized implant for canine cruciate ligament treatment by tibial tuberosity advancement. *Biofabrication.* 2014; 6:025005.doi: 10.1088/1758-5082/6/2/025005 [PubMed: 24658159]
14. Castilho M, Moseke C, Ewald A, Gbureck U, Groll J, Pires I, Tessmar J, Vorndran E. Direct 3D powder printing of biphasic calcium phosphate scaffolds for substitution of complex bone defects. *Biofabrication.* 2014; 6:015006.doi: 10.1088/1758-5082/6/1/015006 [PubMed: 24429776]
15. Castilho M, Rodrigues J, Pires I, Gouveia B, Pereira M, Moseke C, Groll J, Ewald A, Vorndran E. Fabrication of individual alginate-TCP scaffolds for bone tissue engineering by means of powder printing. *Biofabrication.* 2015; 7:015004.doi: 10.1088/1758-5090/7/1/015004 [PubMed: 25562119]
16. Chai YC, Carlier A, Bolander J, Roberts SJ, Geris L, Schrooten J, Van Oosterwyck H, Luyten FP. Current views on calcium phosphate osteogenicity and the translation into effective bone regeneration strategies. *Acta Biomater.* 2012; 8:3876–3887. [PubMed: 22796326]
17. Chow LC. Next generation calcium phosphate-based biomaterials. *Dent Mater J.* 2009; 28:1–10. [PubMed: 19280963]
18. Chu TM, Halloran JW, Hollister SJ, Feinberg SE. Hydroxyapatite implants with designed internal architecture. *J Mater Sci Mater Med.* 2001; 12:471–478. [PubMed: 15348260]
19. Comesana R, Lusquinos F, Del Val J, Quintero F, Riveiro A, Boutinguiza M, Jones JR, Hill RG, Pou J. Toward smart implant synthesis: bonding bioceramics of different resorbability to match bone growth rates. *Sci Rep.* 2015; 5:10677.doi: 10.1038/srep10677 [PubMed: 26032983]
20. Costa PF, Vaquette C, Zhang Q, Reis RL, Ivanovski S, Huttmacher DW. Advanced tissue engineering scaffold design for regeneration of the complex hierarchical periodontal structure. *J Clin Periodontol.* 2014; 41:283–294. DOI: 10.1111/jcpe.12214 [PubMed: 24304192]

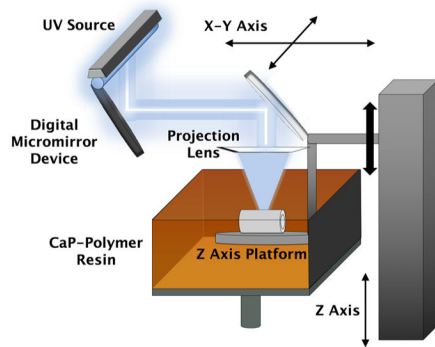
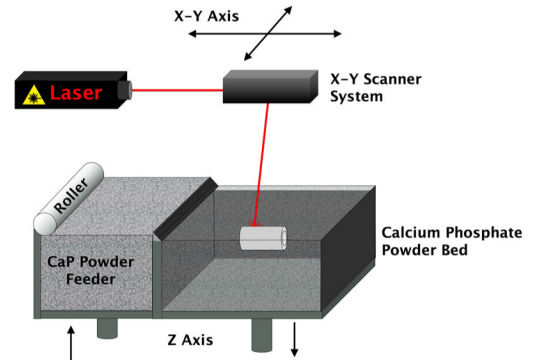
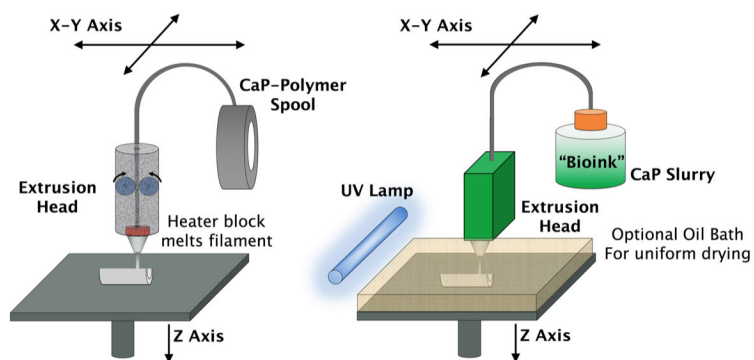
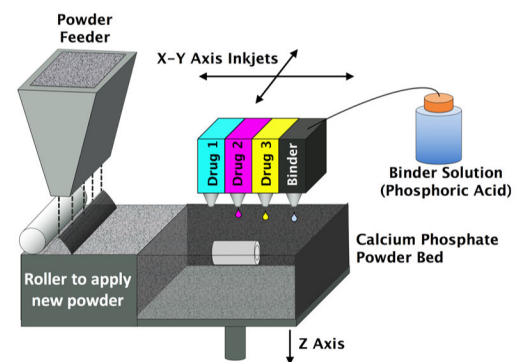
21. Detsch R, Schaefer S, Deisinger U, Ziegler G, Seitz H, Leukers B. In vitro: osteoclastic activity studies on surfaces of 3D printed calcium phosphate scaffolds. *J Biomater Appl.* 2011; 26:359–380. DOI: 10.1177/0885328210373285 [PubMed: 20659962]
22. Detsch R, Uhl F, Deisinger U, Ziegler G. 3D-Cultivation of bone marrow stromal cells on hydroxyapatite scaffolds fabricated by dispense-plotting and negative mould technique. *J Mater Sci Mater Med.* 2008; 19:1491–1496. [PubMed: 17990079]
23. Duan B, Wang M. Customized Ca-P/PHBV nanocomposite scaffolds for bone tissue engineering: design, fabrication, surface modification and sustained release of growth factor. *J R Soc Interface.* 2010; 7(Suppl 5):S615–S629. [PubMed: 20504805]
24. Duan B, Wang M, Zhou WY, Cheung WL, Li ZY, Lu WW. Three-dimensional nanocomposite scaffolds fabricated via selective laser sintering for bone tissue engineering. *Acta Biomater.* 2010; 6:4495–4505. DOI: 10.1016/j.actbio.2010.4406.4024 [PubMed: 20601244]
25. Durucan C, Brown PW. Reactivity of alpha-tricalcium phosphate. *J Mater Sci.* 2002; 37:963–969.
26. El-Ghannam A, Cunningham L Jr, Pienkowski D, Hart A. Bone engineering of the rabbit ulna. *J Oral Maxillofac Surg.* 2007; 65:1495–1502. [PubMed: 17656274]
27. El-Ghannam A, Hart A, White D, Cunningham L. Mechanical properties and cytotoxicity of a resorbable bioactive implant prepared by rapid prototyping technique. *J Biomed Mater Res A.* 2013; 101:2851–2861. [PubMed: 23504981]
28. El-Ghannam A, Ning CQ, Mehta J. Cyclosilicate nanocomposite: a novel resorbable bioactive tissue engineering scaffold for BMP and bone-marrow cell delivery. *J Biomed Mater Res A.* 2004; 71:377–390. [PubMed: 15470721]
29. Fielding G, Bose S. SiO₂ and ZnO dopants in three-dimensionally printed tricalcium phosphate bone tissue engineering scaffolds enhance osteogenesis and angiogenesis in vivo. *Acta Biomater.* 2013; 9:9137–9148. DOI: 10.1016/j.actbio.2013.9107.9009 [PubMed: 23871941]
30. Fu Q, Saiz E, Tomsia AP. Direct ink writing of highly porous and strong glass scaffolds for load-bearing bone defects repair and regeneration. *Acta Biomater.* 2011; 7:3547–3554. [PubMed: 21745606]
31. Gao Y, Cao WL, Wang XY, Gong YD, Tian JM, Zhao NM, Zhang XF. Characterization and osteoblast-like cell compatibility of porous scaffolds: bovine hydroxyapatite and novel hydroxyapatite artificial bone. *J Mater Sci Mater Med.* 2006; 17:815–823. [PubMed: 16932863]
32. Gao G, Schilling AF, Yonezawa T, Wang J, Dai G, Cui X. Bioactive nanoparticles stimulate bone tissue formation in bioprinted three-dimensional scaffold and human mesenchymal stem cells. *Biotechnol J.* 2014; 9:1304–1311. [PubMed: 25130390]
33. Gbureck U. Mechanical activation and cement formation of β -tricalcium phosphate. *Biomaterials.* 2003; 24:4123–4131. [PubMed: 12853242]
34. Gbureck U, Hölzel T, Doillon CJ, Müller FA, Barralet JE. Direct printing of bioceramic implants with spatially localized angiogenic factors. *Adv Mater.* 2007; 19:795–800.
35. Gbureck U, Hölzel T, Klammert U, Würzler K, Müller FA, Barralet JE. Resorbable dicalcium phosphate bone substitutes prepared by 3D powder printing. *Adv Funct Mater.* 2007; 17:3940–3945.
36. Gbureck U, Vorndran E, Barralet JE. Modeling vancomycin release kinetics from microporous calcium phosphate ceramics comparing static and dynamic immersion conditions. *Acta Biomater.* 2008; 4:1480–1486. [PubMed: 18485844]
37. Gbureck U, Vorndran E, Muller FA, Barralet JE. Low temperature direct 3D printed bioceramics and biocomposites as drug release matrices. *J Control Release.* 2007; 122:173–180. [PubMed: 17655962]
38. Gerstenfeld LC, Cho TJ, Kon T, Aizawa T, Tsay A, Fitch J, Barnes GL, Graves DT, Einhorn TA. Impaired fracture healing in the absence of TNF-alpha signaling: the role of TNF-alpha in endochondral cartilage resorption. *J Bone Miner Res.* 2003; 18:1584–1592. [PubMed: 12968667]
39. Habibovic P, Gbureck U, Doillon CJ, Bassett DC, van Blitterswijk CA, Barralet JE. Osteoconduction and osteoinduction of low-temperature 3D printed bioceramic implants. *Biomaterials.* 2008; 29:944–953. [PubMed: 18055009]

40. He HY, Zhang JY, Mi X, Hu Y, Gu XY. Rapid prototyping for tissue-engineered bone scaffold by 3D printing and biocompatibility study. *Int J Clin Exp Med*. 2015; 8:11777–11785. [PubMed: 26380018]
41. Hull CW. Apparatus for production of three-dimensional objects by stereolithography. Google Patents. 1986
42. Igawa K, Mochizuki M, Sugimori O, Shimizu K, Yamazawa K, Kawaguchi H, Nakamura K, Takato T, Nishimura R, Suzuki S, Anzai M, Chung UI, Sasaki N. Tailor-made tricalcium phosphate bone implant directly fabricated by a three-dimensional ink-jet printer. *J Artif Organs*. 2006; 9:234–240. [PubMed: 17171402]
43. Inzana JA, Olvera D, Fuller SM, Kelly JP, Graeve OA, Schwarz EM, Kates SL, Awad HA. 3D printing of composite calcium phosphate and collagen scaffolds for bone regeneration. *Biomaterials*. 2014; 35:4026–4034. DOI: 10.1016/j.biomaterials.2014.4001.4064 [PubMed: 24529628]
44. Inzana JA, Trombetta RP, Schwarz EM, Kates SL, Awad HA. 3D printed bioceramics for dual antibiotic delivery to treat implant-associated bone infection. *Eur Cell Mater*. 2015; 30:232–247. [PubMed: 26535494]
45. Ishack S, Mediero A, Wilder T, Ricci JL, Cronstein BN. Bone regeneration in critical bone defects using three-dimensionally printed beta-tricalcium phosphate/hydroxyapatite scaffolds is enhanced by coating scaffolds with either dipyrnidamole or BMP-2. *J Biomed Mater Res B Appl Biomater*. 2015; doi: 10.1002/jbm.b.33561
46. Johnsson MS, Nancollas GH. The role of brushite and octacalcium phosphate in apatite formation. *Crit Rev Oral Biol Med*. 1992; 3:61–82. [PubMed: 1730071]
47. Kalita SJ, Bose S, Hosick HL, Bandyopadhyay A. Development of controlled porosity polymer-ceramic composite scaffolds via fused deposition modeling. *Mater Sci Eng C*. 2003; 23:611–620.
48. Kang HW, Lee SJ, Ko IK, Kengla C, Yoo JJ, Atala A. A 3D bioprinting system to produce human-scale tissue constructs with structural integrity. *Nat Biotechnol*. 2016; 34(3):312–319. [PubMed: 26878319]
49. Khalyfa A, Vogt S, Weisser J, Grimm G, Rechtenbach A, Meyer W, Schnabelrauch M. Development of a new calcium phosphate powder-binder system for the 3D printing of patient specific implants. *J Mater Sci Mater Med*. 2007; 18:909–916. [PubMed: 17216579]
50. Kim J, McBride S, Tellis B, Alvarez-Urea P, Song YH, Dean DD, Sylvia VL, Elgendy H, Ong J, Hollinger JO. Rapid-prototyped PLGA/beta-TCP/hydroxyapatite nanocomposite scaffolds in a rabbit femoral defect model. *Biofabrication*. 2012; 4:025003. [PubMed: 22427485]
51. Kim K, Yeatts A, Dean D, Fisher JP. Stereolithographic bone scaffold design parameters: osteogenic differentiation and signal expression. *Tissue Eng B Rev*. 2010; 16:523–539.
52. Klammert U, Vorndran E, Reuther T, Muller FA, Zorn K, Gbureck U. Low temperature fabrication of magnesium phosphate cement scaffolds by 3D powder printing. *J Mater Sci Mater Med*. 2010; 21:2947–2953. [PubMed: 20740307]
53. Komlev VS, Popov VK, Mironov AV, Fedotov AY, Teterina AY, Smirnov IV, Bozo IY, Rybko VA, Deev RV. 3D printing of octacalcium phosphate bone substitutes. *Front Bioeng Biotechnol*. 2015; 3:81. doi: 10.3389/fbioe.2015.00081 [PubMed: 26106596]
54. Lam CX, Hutmacher DW, Schantz JT, Woodruff MA, Teoh SH. Evaluation of polycaprolactone scaffold degradation for 6 months in vitro and in vivo. *J Biomed Mater Res A*. 2009; 90:906–919. [PubMed: 18646204]
55. Lee JW, Ahn G, Kim DS, Cho DW. Development of nano- and microscale composite 3D scaffolds using PPF/DEF-HA and micro-stereolithography. *Microelectron Eng*. 2009; 86:1465–1467.
56. Lee JW, Kang KS, Lee SH, Kim JY, Lee BK, Cho DW. Bone regeneration using a microstereolithography-produced customized poly(propylene fumarate)/di-ethyl fumarate photopolymer 3D scaffold incorporating BMP-2 loaded PLGA microspheres. *Biomaterials*. 2011; 32:744–752. [PubMed: 20933279]
57. Lee KW, Wang S, Fox BC, Ritman EL, Yaszemski MJ, Lu L. Poly(propylene fumarate) bone tissue engineering scaffold fabrication using stereolithography: effects of resin formulations and laser parameters. *Biomacromolecules*. 2007; 8:1077–1084. [PubMed: 17326677]

58. Lee KW, Wang S, Yaszemski MJ, Lu L. Physical properties and cellular responses to crosslinkable poly(propylene fumarate)/hydroxyapatite nanocomposites. *Biomaterials*. 2008; 29:2839–2848. [PubMed: 18403013]
59. Liao HT, Chen YY, Lai YT, Hsieh MF, Jiang CP. The osteogenesis of bone marrow stem cells on mPEG-PCL-mPEG/hydroxyapatite composite scaffold via solid freeform fabrication. *Biomed Res Int*. 2014; 2014:321549. [PubMed: 24868523]
60. Liao HT, Lee MY, Tsai WW, Wang HC, Lu WC. Osteogenesis of adipose-derived stem cells on polycaprolactone-beta-tricalcium phosphate scaffold fabricated via selective laser sintering and surface coating with collagen type I. *J Tissue Eng Regen Med*. 2013; doi: 10.1002/term.1811
61. Lode A, Meissner K, Luo Y, Sonntag F, Glorius S, Nies B, Vater C, Despong F, Hanke T, Gelinsky M. Fabrication of porous scaffolds by three-dimensional plotting of a pasty calcium phosphate bone cement under mild conditions. *J Tissue Eng Regen Med*. 2014; 8:682–693. DOI: 10.1002/term.1563 [PubMed: 22933381]
62. Luo Y, Wu C, Lode A, Gelinsky M. Hierarchical mesoporous bioactive glass/alginate composite scaffolds fabricated by three-dimensional plotting for bone tissue engineering. *Biofabrication*. 2013; 5:015005. [PubMed: 23228963]
63. Mangano C, Barboni B, Valbonetti L, Berardinelli P, Martelli A, Muttini A, Bedini R, Tete S, Piattelli A, Mattioli M. In vivo behavior of a custom-made 3D synthetic bone substitute in sinus augmentation procedures in sheep. *J Oral Implantol*. 2015; 41:240–250. DOI: 10.1563/AAID-JO-I-D-1513-00053 [PubMed: 23829685]
64. Martinez-Vazquez FJ, Cabanas MV, Paris JL, Lozano D, Vallet-Regi M. Fabrication of novel Si-doped hydroxyapatite/gelatine scaffolds by rapid prototyping for drug delivery and bone regeneration. *Acta Biomater*. 2015; 15:200–209. DOI: 10.1016/j.actbio.2014.1012.1021 [PubMed: 25560614]
65. Mehrban N, Bowen J, Vorndran E, Gbureck U, Grover LM. Structural changes to resorbable calcium phosphate bioceramic aged in vitro. *Colloids Surf B Biointerfaces*. 2013; 111:469–478. DOI: 10.1016/j.colsurfb.2013.1006.1020 [PubMed: 23876446]
66. Mountziaris PM, Spicer PP, Kasper FK, Mikos AG. Harnessing and modulating inflammation in strategies for bone regeneration. *Tissue Eng B Rev*. 2011; 17:393–402.
67. Murphy SV, Atala A. 3D bioprinting of tissues and organs. *Nat Biotechnol*. 2014; 32:773–785. [PubMed: 25093879]
68. Nandakumar A, Cruz C, Mentink A, Tahmasebi Birgani Z, Moroni L, van Blitterswijk C, Habibovic P. Monolithic and assembled polymer-ceramic composites for bone regeneration. *Acta Biomater*. 2013; 9:5708–5717. DOI: 10.1016/j.actbio.2012.5710.5044 [PubMed: 23142480]
69. Poldervaart MT, Gremmels H, van Deventer K, Fledderus JO, Oner FC, Verhaar MC, Dhert WJ, Alblas J. Prolonged presence of VEGF promotes vascularization in 3D bioprinted scaffolds with defined architecture. *J Controlled Release*. 2014; 184:58–66.
70. Poldervaart MT, Wang H, van der Stok J, Weinans H, Leeuwenburgh SC, Oner FC, Dhert WJ, Alblas J. Sustained release of BMP-2 in bioprinted alginate for osteogenicity in mice and rats. *PLoS One*. 2013; 8:e72610. doi: 10.1371/journal.pone.0072610 [PubMed: 23977328]
71. Rath SN, Strobel LA, Arkudas A, Beier JP, Maier AK, Greil P, Horch RE, Kneser U. Osteoinduction and survival of osteoblasts and bone-marrow stromal cells in 3D biphasic calcium phosphate scaffolds under static and dynamic culture conditions. *J Cell Mol Med*. 2012; 16:2350–2361. [PubMed: 22304383]
72. Seol YJ, Park JY, Jung JW, Jang J, Girdhari R, Kim SW, Cho DW. Improvement of bone regeneration capability of ceramic scaffolds by accelerated release of their calcium ions. *Tissue Eng A*. 2014; 20:2840–2849. DOI: 10.1089/ten.TEA.2012.0726
73. Serra T, Planell JA, Navarro M. High-resolution PLA-based composite scaffolds via 3-D printing technology. *Acta Biomater*. 2013; 9:5521–5530. [PubMed: 23142224]
74. Seyednejad H, Gawlitta D, Kuiper RV, de Bruin A, van Nostrum CF, Vermonden T, Dhert WJ, Hennink WE. In vivo biocompatibility and biodegradation of 3D-printed porous scaffolds based on a hydroxyl-functionalized poly(epsilon-caprolactone). *Biomaterials*. 2012; 33:4309–4318. [PubMed: 22436798]

75. Shim JH, Kim SE, Park JY, Kundu J, Kim SW, Kang SS, Cho DW. Three-dimensional printing of rhBMP-2-loaded scaffolds with long-term delivery for enhanced bone regeneration in a rabbit diaphyseal defect. *Tissue Eng A*. 2014; 20:1980–1992.
76. Shuai C, Li P, Liu J, Peng S. Optimization of TCP/HAP ratio for better properties of calcium phosphate scaffold via selective laser sintering. *Mater Charact*. 2013; 77:23–31.
77. Sobral JM, Caridade SG, Sousa RA, Mano JF, Reis RL. Three-dimensional plotted scaffolds with controlled pore size gradients: effect of scaffold geometry on mechanical performance and cell seeding efficiency. *Acta Biomater*. 2011; 7:1009–1018. [PubMed: 21056125]
78. Strobel LA, Rath SN, Maier AK, Beier JP, Arkudas A, Greil P, Horch RE, Kneser U. Induction of bone formation in biphasic calcium phosphate scaffolds by bone morphogenetic protein-2 and primary osteoblasts. *J Tissue Eng Regen Med*. 2014; 8:176–185. DOI: 10.1002/term.1511 [PubMed: 22740314]
79. Suwanprateeb J, Suvannapruk W, Wasoontararat K. Low temperature preparation of calcium phosphate structure via phosphorization of 3D-printed calcium sulfate hemihydrate based material. *J Mater Sci Mater Med*. 2010; 21:419–429. DOI: 10.1007/s10856-10009-13883-10851 [PubMed: 19784760]
80. Sweet L, Kang Y, Czisch C, Witek L, Shi Y, Smay J, Plant GW, Yang Y. Geometrical versus random beta-TCP scaffolds: exploring the effects on Schwann Cell growth and behavior. *PLoS One*. 2015; 10:e0139820. doi: 10.1371/journal.pone.0139820 [PubMed: 26444999]
81. Tamimi F, Torres J, Al-Abedalla K, Lopez-Cabarcos E, Alkhraisat MH, Bassett DC, Gbureck U, Barralet JE. Osseointegration of dental implants in 3D-printed synthetic onlay grafts customized according to bone metabolic activity in recipient site. *Biomaterials*. 2014; 35:5436–5445. DOI: 10.1016/j.biomaterials.2014.5403.5050 [PubMed: 24726538]
82. Thomas MV, Puleo DA. Calcium sulfate: properties and clinical applications. *J Biomed Mater Res B Appl Biomater*. 2009; 88:597–610. [PubMed: 19025981]
83. Torres J, Tamimi F, Alkhraisat MH, Prados-Frutos JC, Rastikerdar E, Gbureck U, Barralet JE, Lopez-Cabarcos E. Vertical bone augmentation with 3D-synthetic monetite blocks in the rabbit calvaria. *J Clin Periodontol*. 2011; 38:1147–1153. DOI: 10.1111/j.1600-1051X.2011.01787.x [PubMed: 22092695]
84. Tumbleston JR, Shirvanyants D, Ermoshkin N, Januszewicz R, Johnson AR, Kelly D, Chen K, Pinschmidt R, Rolland JP, Ermoshkin A, Samulski ET, DeSimone JM. Additive manufacturing Continuous liquid interface production of 3D objects. *Science*. 2015; 347:1349–1352. [PubMed: 25780246]
85. Van der Stok J, Van der Jagt OP, Amin Yavari S, De Haas MF, Waarsing JH, Jahr H, Van Lieshout EM, Patka P, Verhaar JA, Zadpoor AA, Weinans H. Selective laser melting-produced porous titanium scaffolds regenerate bone in critical size cortical bone defects. *J Orthop Res*. 2013; 31:792–799. [PubMed: 23255164]
86. van der Stok J, Wang H, Amin Yavari S, Siebelt M, Sandker M, Waarsing JH, Verhaar JA, Jahr H, Zadpoor AA, Leeuwenburgh SC, Weinans H. Enhanced bone regeneration of cortical segmental bone defects using porous titanium scaffolds incorporated with colloidal gelatin gels for time- and dose-controlled delivery of dual growth factors. *Tissue Eng A*. 2013; 19:2605–2614.
87. Wang S, Kempen DH, Simha NK, Lewis JL, Windebank AJ, Yaszemski MJ, Lu L. Photo-cross-linked hybrid polymer networks consisting of poly(propylene fumarate) and poly(caprolactone fumarate): controlled physical properties and regulated bone and nerve cell responses. *Biomacromolecules*. 2008; 9:1229–1241. [PubMed: 18307311]
88. Wang S, Kempen DH, Yaszemski MJ, Lu L. The roles of matrix polymer crystallinity and hydroxyapatite nanoparticles in modulating material properties of photo-crosslinked composites and bone marrow stromal cell responses. *Biomaterials*. 2009; 30:3359–3370. [PubMed: 19339048]
89. Wang J, Yang M, Zhu Y, Wang L, Tomsia AP, Mao C. Phage nanofibers induce vascularized osteogenesis in 3D printed bone scaffolds. *Adv Mater*. 2014; 26:4961–4966. DOI: 10.1002/adma.201400154 [PubMed: 24711251]
90. Wang S, Yaszemski MJ, Gruetzmacher JA, Lu L. Photo-crosslinked poly(epsilon-caprolactone fumarate) networks: roles of crystallinity and crosslinking density in determining mechanical properties. *Polymer (Guildf)*. 2008; 49:5692–5699. [PubMed: 20936057]

91. Warnke PH, Seitz H, Warnke F, Becker ST, Sivananthan S, Sherry E, Liu Q, Wiltfang J, Douglas T. Ceramic scaffolds produced by computer-assisted 3D printing and sintering: characterization and biocompatibility investigations. *J Biomed Mater Res B Appl Biomater*. 2010; 93:212–217. DOI: 10.1002/jbm.b.31577 [PubMed: 20091914]
92. Will J, Melcher R, Treul C, Travitzky N, Kneser U, Polykandriotis E, Horch R, Greil P. Porous ceramic bone scaffolds for vascularized bone tissue regeneration. *J Mater Sci Mater Med*. 2008; 19:2781–2790. DOI: 10.1007/s10856-10007-13346-10855 [PubMed: 18305907]
93. Williams JM, Adewunmi A, Schek RM, Flanagan CL, Krebsbach PH, Feinberg SE, Hollister SJ, Das S. Bone tissue engineering using polycaprolactone scaffolds fabricated via selective laser sintering. *Biomaterials*. 2005; 26:4817–4827. [PubMed: 15763261]
94. Wu C, Luo Y, Cuniberti G, Xiao Y, Gelinsky M. Three-dimensional printing of hierarchical and tough mesoporous bioactive glass scaffolds with a controllable pore architecture, excellent mechanical strength and mineralization ability. *Acta Biomater*. 2011; 7:2644–2650. [PubMed: 21402182]
95. Xia Y, Zhou P, Cheng X, Xie Y, Liang C, Li C, Xu S. Selective laser sintering fabrication of nano-hydroxyapatite/poly-epsilon-caprolactone scaffolds for bone tissue engineering applications. *Int J Nanomed*. 2013; 8:4197–4213.
96. Yang X, Ricciardi BF, Hernandez-Soria A, Shi Y, Pleshko Camacho N, Bostrom MP. Callus mineralization and maturation are delayed during fracture healing in interleukin-6 knockout mice. *Bone*. 2007; 41:928–936. [PubMed: 17921078]
97. Yang S, Wang J, Tang L, Ao H, Tan H, Tang T, Liu C. Mesoporous bioactive glass doped-poly (3-hydroxybutyrate-co-3-hydroxyhexanoate) composite scaffolds with 3-dimensionally hierarchical pore networks for bone regeneration. *Colloids Surf B Biointerfaces*. 2014; 116:72–80. [PubMed: 24441182]
98. Zhang Y, Xia L, Zhai D, Shi M, Luo Y, Feng C, Fang B, Yin J, Chang J, Wu C. Mesoporous bioactive glass nanolayer-functionalized 3D-printed scaffolds for accelerating osteogenesis and angiogenesis. *Nanoscale*. 2015; 7:19207–19221. DOI: 10.11039/c19205nr05421d [PubMed: 26525451]
99. Zhou Z, Buchanan F, Mitchell C, Dunne N. Printability of calcium phosphate: calcium sulfate powders for the application of tissue engineered bone scaffolds using the 3D printing technique. *Mater Sci Eng C Mater Biol Appl*. 2014; 38:1–10. [PubMed: 24656346]

(a) Vat Polymerization**(b) Powder Bed Fusion****(c) Material Extrusion****(d) Binder Jetting****FIGURE 1.**

Schematic depiction of the major technologies used in 3D printing of pure or composite calcium phosphate scaffolds for bone regeneration and drug delivery.

TABLE 1

Overview of the reviewed 3D printing processes for bone scaffolds.

3D printing technology	Materials for bone tissue engineering*	Fabrication resolution	Advantages	Disadvantages
Vat Polymerization	PPF, PCLF, PPF/PCLF, urethane acrylate monomer. Resins supplemented with HA or TCP	500 nm – 101.6 μm^a	Fine resolution, ability to incorporate bioactive molecules within polymer	Limited ratio of ceramic additives to photocurable polymer
Powder Bed Fusion	PCL, HA, biphasic CaP, polymer/CaP composites, CaP nanoparticles encapsulated in PHBV microspheres	150 – 800 μm^b	High strength scaffolds, wide range of materials	Thermal binding disallows incorporation of growth factors and/or drugs
Material Extrusion	Polyesters, synthetic polymers (i.e., PEG-PLA, PCL, etc.) natural polymers (i.e., alginate, chitosan, etc.), CaP slurries, PMMA, polymer/ceramic (including bioactive glass) composites, photocurable hydrogels (i.e., PEGDMA), cell suspensions in hydrogels	200 – 838 μm^c	Wide range of materials and extrusion techniques, ability to print bioactive molecules or live-cell suspensions in “bioinks”	Most require post-fabrication treatment (i.e., sintering, immersion in crosslinking agent, etc.)
Binder Jetting	HA, TCP, other CaPs (i.e., calcium carbonate, tetracalcium phosphate, octacalcium phosphate etc.)	50 – 300 μm^a	Ability to print pure CaP scaffolds, simultaneous printing of bioinks (drugs or growth factors) in ink cartridges	Designed pores limited to ~ 500 μm , brittle and limited mechanical properties, inability to directly print cells

The asterisk (*) reflects that the materials listed in this table are limited to those used in the cited papers.

PPF: poly(propylene fumarate), PCLF: poly(*ε*-caprolactone fumarate), HA: hydroxyapatite, TCP: tricalcium phosphate, PCL: poly(*ε*-caprolactone), CaP: calcium phosphate, PHBV: poly(hydroxybutyrate-co-hydroxyvalerate), PEG: polyethylene glycol, PLA: polylactic acid, PMMA: polymethylmethacrylate, PEGDMA: poly(ethylene glycol)dimethacrylate.

^aDefined by layer thickness.

^bDefined by laser diameter.

^cDefined by nozzle diameter.

TABLE 2Calcium phosphates relevant to bone regeneration.^{8,10,16,17}

Name	Formula	Ca:P ratio	Solubility ($\sim K_{sp}$)
Hydroxyapatite (HA)	$Ca_{10}(PO_4)_6(OH)_2$	1.67	10^{-120}
Tricalcium phosphate (TCP)	$Ca_3(PO_4)_2$	1.5	α .5 cal 10^{-25} β 25 cal 10^{-29}
Tetracalcium phosphate (TTCP)	$Ca_4(PO_4)_2O$	2.0	10^{-44} – 10^{-38}
Dicalcium phosphate dihydrate (DCPD; Brushite)	$CaHPO_4 \cdot 2H_2O$	1.0	$10^{-6.6}$
Dicalcium phosphate anhydrous (DCPA; Monetite)	$CaHPO_4$	1.0	$10^{-6.9}$
Octacalcium phosphate (OCP)	$Ca_8H_2(PO_4)_6 \cdot 5H_2O$	1.33	10^{-97}
Calcium pyrophosphate (CPP)	$Ca_2P_2O_7$	1.0	10^{-15}

Author Manuscript

Author Manuscript

Author Manuscript

Author Manuscript

TABLE 3

Low-temperature 3D printing for bone regeneration.

Reference	3D printing technology	Printed material(s)	Post-processing	Cells/animal model	Primary findings
<i>In vitro</i> studies					
Almeida, 2014	Material extrusion	Two bioinks: 1 PEG-PLA + BG (G5) 2 Chitosan	PEG-PLA/G5: cross-linked with NaOH (8% w/v) in ethanol (70%) drop wise during printing Chitosan: Overnight gelation	Human monocytes	PEG-PLA/G5 scaffolds upregulated IL-6,12/23,10. Chitosan scaffolds upregulated TNF- α . Geometry (larger pores and wider angles) increased TNF- α and IL-12/23 ²
Gao, 2014	Binder jetting	PEGDMA \pm BG \pm HA	UV photo polymerization during the printing process	hMSCs	PEGDMA-HA increased cell viability and osteogenic differentiation (ALP activity and Col10A1 gene expression) and increased compressive modulus compared to PEGDMA-BG or PEGDMA-BG-HA ³²
Lode, 2014	Material extrusion	α -TCP paste in biocompatible oil (short-chain triglyceride)	Reaction setting in water followed by incubation at 37°C	hMSCs	Osteogenically-induced hMSCs-seeded scaffolds demonstrated favorable cytocompatibility and osteogenic differentiation compared to native cells ⁶¹
Castilho, 2015	Binder jetting	CaP Powder: α/β -TCP Binder: 20% H ₃ PO ₄	Binder dip followed by PBS washes and vacuum infiltration with alginate at 37°C	MG63 OB cells	Significant increase in mechanics of alginate-modified scaffolds, coupled with improvement of OB cells proliferation and cell viability ¹⁵
Mehrban, 2013	Binder jetting	CaP Powder: TCP Binder: 20% H ₃ PO ₄	Triplicate 30 s immersions in binder	Rat tenocytes	Sera proteins strongly increased the rate of degradation and increased pore diameters in the scaffold. Presence of tenocytes inhibited increase in scaffold porosity ⁶⁵
<i>In vivo</i> studies					
Castilho, 2014	Binder jetting	CaP Powder: α/β -TCP Binder: 20% H ₃ PO ₄	30 s immersion in binder	Canine tibia tuberosity advancement (TTA)	Use of 3D printed bioceramic cage to treat CrCL crucial ligament deficient stifle by TTA enabled complete limb function restoration without adverse complications or patient lameness compared to standard titanium cage technique ¹³
Habibovic, 2008	Binder jetting	CaP Powder: α/β -TCP Binder: 20% H ₃ PO ₄	Triplicate 30 s immersions in binder followed by autoclaving	Goat decorticated lumbar or intramuscular implants	Orthotopic implants facilitated bone formation into pores and ectopic implants had thin layers of bone on the implant surfaces ³⁹
Igawa, 2006	Binder jetting	CaP Powder: α -TCP Binder: 5% sodium chondroitin sulfate, 12% disodium succinate, 83% DI water	None	Canine cranial defect	Bone growth occurred into the macropores of 3D-printed scaffolds. 3D-printed CaP had faster bone resorption and better integration compared with HA scaffolds ⁴²

Reference	3D printing technology	Printed material(s)	Post-processing	Cells/animal model	Primary findings
Inzana, 2014	Binder jetting	CaP Powder: α -TCP/HA Binder: 8.75% H_3PO_4 + 0.25% Tween 80 \pm collagen	Flash dip in 0.1% H_3PO_4 followed by triplicate 120 s washes in H_2O	Mouse femoral defect	Collagen-CaP composite scaffolds demonstrated enhanced material properties and <i>in vitro</i> cell cytocompatibility. <i>In vivo</i> , CaP scaffolds demonstrated osteoconductivity but healing of critical defect was incomplete regardless of collagen infiltration or coating ⁴³
Komlev, 2015	Binder jetting	CaP Powder: TCP Binder: 1% H_3PO_4	7-day immersion in $NH_4H_2PO_4$ followed by 7-day immersion in CH_3COONa at 40°C and air drying	Rabbit cranial defect	2.5-fold increase in peripheral bone ingrowth compared to native repair at 6.5 months ⁵³

PEG poly(ethylene glycol), PLA poly(lactic acid), TCP tricalcium phosphate, CaP calcium phosphate, *TCP* tricalcium phosphate, *HA* hydroxyapatite, *IL* interleukin, *TNF- α* tumor necrosis factor α , *PEGDMA* poly(-ethylene glycol) dimethacrylate, *BG* bioactive glass, *hMSCs* human mesenchymal stem cells.

TABLE 4

High-temperature 3D printing for bone regeneration—*in vitro* experiments.

Reference	3D printing technology	Printed material(s)	Post-processing	Cells/animal model	Primary findings
Gao, 2006	Material Extrusion	HA slurry laminated with 4% alginate	Heated to 300–500°C, followed by sintering at 1150°C	Pre-OB cell line MC3T3-E1	Scaffolds provided good attachment, proliferation and differentiation of OB cells ³¹
Nandakumar, 2013	Material extrusion	Filaments of polyActive™ (PA), PEOT/PBT co-polymer, and HA ceramic	Extruded at a temperature between 195 and 210°C	hMSCs	PA-HA composite scaffolds increased metabolic activity of cells and enhanced osteogenic differentiation (Osteopontin expression) ⁶⁸
Sweet, 2015	Material extrusion	β -TCP slurry (Surfonal surfactant, Darvan C dispersant and carboxymethyl cellulose powder)	Sintered 1250°C	Rat Schwann cells (SC)	β -TCP scaffolds can support the growth of SC with spindle cell morphologies and improved alignment. Scaffolds also induced distinct neural and angiogenic growth factor expression in 3D culture condition ⁸⁰
Detsch, 2011	Binder jetting	HA, TCP, or HA/TCP (60/40) Binder: Not specified	Sintered at 1300°C	RAW 264.7 OC cell line	OC-like cells able to resorb calcium phosphate surfaces ²¹
Bergemann, 2016	Binder jetting	CaP Powder: β -TCP Binder: dextrin + saccharose	Sintered at 1250°C then infiltrated by PLA. Amino group surface modification by plasma or by PPAAm processes	Human MG-63 OB cell line	Dynamic cell culture of the PPAAm PLA-CaP scaffold enabled efficient cell colonization, leading to pervasive cellularity within 14 days ⁷
Castilho, 2014	Binder jetting	CaP Powder: TCP, HA, and BCB (TCP/HA) of different ratios) Binder: 10% H ₃ PO ₄	Sintered at 1200°C	Human MG-63 OB cell line	All BCP cytocompatible and had enhanced cell proliferation compared to pure TCP and HA scaffolds ¹⁴
Khalyfa, 2007	Binder jetting	CaP Powder: TTCP + (β -TCP or Calcium sulfate dihydrate) Binder: Citric Acid	Either sintering at 1000, 1200, and 1400°C or infiltrated with polymer and cured at 110°C	Pre-OB cell line MC3T3-E1	Physical characterization and cytocompatibility experiments indicate β -TCP/TTCP 3D printed scaffolds are suitable for bone substitutes and grafts as evident by adherent cell growth and alkaline phosphatase activity ⁴⁹
Rath, 2012	Binder jetting	CaP Powder: β -TCP + HA + potato starch powder (dextrin) Binder: Water-glycerol	Sintered at 1200 °C	Rat MSCs	Scaffold cytocompatibility evident by increased proliferation in static culture conditions. Osteogenic induction and hydrodynamic bioreactor cultivation reduces proliferation and enhances osteogenic differentiation ⁷¹
Warnke, 2010	Binder jetting	CaP Powder: TCP and HA Binder: polymeric binder (Schelofix)	Sintered at 1250°C	Primary hOB	Both versions of 3D printed and sintered scaffolds were colonized by human osteoblasts, however more cells were seen on HAP scaffolds than TCP scaffolds. Cytocompatibility HA > BioOss® > TCP ⁹¹
Duan, 2010	Powder bed fusion	CaP/PHBV microspheres or CHAP/PLLA microspheres	None	SaOS-2 OB cell line	Incorporation of CaP nanoparticles significantly improved cell proliferation and alkaline phosphatase activity for PHBV-based scaffolds, whereas CHAP/PLLA nanocomposite scaffolds exhibited a similar level of cell response compared with PLLA polymer scaffolds ²⁴

Reference	3D printing technology	Printed material(s)	Post-processing	Cells/animal model	Primary findings
Comesana, 2015	Powder bed fusion	Microspheres of multiphasic CaP coated with bioactive glass (45S5)	None	Pre-OB cell line MC3T3-E1	Scaffold cytocompatibility demonstrated by absence of toxicity, and MC3T3-E1 cell adherence and proliferation ¹⁹

HA hydroxyapatite, *TCP* tricalcium phosphate, *TTCP* tetracalcium phosphate, *BCB* biphasic calcium carbonate, *OC* osteoclasts, *OB* osteoblasts, *PEOT/PBT* poly(ethylene oxide terephthalate)/poly(butylene terephthalate), *hMSCs* human mesenchymal stem cells, *PPAAM* plasma-polymerized allylamine, *PLA* poly(lactic acid), *PHBV* poly(hydroxybutyrate-co-hydroxyvalerate), *CHAp* carbonated hydroxyapatite, *PLLA* poly(L-lactic acid).

TABLE 5

High-temperature 3D printing for bone regeneration—*in vivo* experiments.

Reference	3D printing technology	Printed material(s)	Post-processing	Cells/growth factor	Animal model	Primary findings
Barboni, 2013	Material extrusion	β -TCP + HA slurry in a binder/dispersant of organic additives	Sintered 1250 °C	oAEC	Sheep sinus augmentation	oAEC seeded on scaffold demonstrated enhanced osteogenesis and angiogenesis, reduced fibrotic reaction and inflammation ⁴
Costa, 2014	Material extrusion	PCL filaments containing 20 wt.% β -TCP	Coated with CaP, press fitted to electrospun PCL component	Ovine OB and PDL cells	Rat subcutaneous implantation	Scaffolds cultured in osteogenic media increased mineralization ALP activity <i>in vitro</i> , and stimulated more bone formation <i>In vivo</i> . Cell sheets enabled attachment to the dentin block and vascularity ²⁰
He, 2015	Material extrusion	PVA + calcined goat spongy bone + biphasic ceramic powder	Dried overnight at 40 °C, then heated to 150 °C	rabbit MSCs	Rabbit	Biocompatibility was confirmed by negative results from acute toxicity, pyrogenic, and intracutaneous stimulation tests in rabbits. <i>In vitro</i> testing showed that MSCs grew and proliferated on scaffold ⁴⁰
Mangano, 2015	Material Extrusion	β -TCP + HA slurry in a binder/dispersant system of organic additives	Sintered at 1250 °C		Sheep sinus augmentation	Scaffold demonstrated good osteoconductive properties and high biocompatibility with the bone regeneration proceeding from the periphery of the scaffold near the points of the contact with the native bone ⁶³
Wang, 2014	Material extrusion	Ceramic slurry of HA- β -TCP in Pluronic F-127	Heated to 600 and 1100 °C and subsequently immersed in VAM	Rat MSCs	Rat radial defect	VAM-MSC-Chitosan 3D printed scaffold induced endothelialization. Implantation of MSC-seeded VAM containing the RGD-phage nanofibers induced bone formation compared to negative controls. Addition of VEGF improved out-come ⁸⁹
Zhang, 2015	Material extrusion	β -TCP-PVA paste with or without mesoporous bioactive glass (MBG) coating	Sintered 1100 °C and then annealed at 650 °C following MBG coating	Rabbit MSCs	Rabbit calvaria defect	Enhanced bone regeneration and angiogenesis in a rabbit calvarial defect model

Reference	3D printing technology	Printed material(s)	Post-processing	Cells/growth factor	Animal model	Primary findings
Fielding, 2013	Binder jetting	CaP Powder: β -TCP doped with ZnO + SiO ₂ Binder: organic water-based binder	Sintered at 1250 °C		Rat Femur Defect	compared to non-coated scaffolds ⁹⁸ Addition of dopants into TCP increased bone formation (collagen I and osteocalcin production) and neovascularization compared to pure TCP scaffolds ²⁹
Tamimi, 2014	Binder jetting	CaP Powder: β -TCP Binder: 20% H ₃ P ₀ ₄	Triplicate immersions in binder followed by autoclaving		Rabbit calvaria defects	Macropores geometry can enhance bone growth, and Ti implant osseointegration within the scaffold ⁸¹
Torres, 2011	Binder jetting	CaP Powder: β -TCP Binder: 20% H ₃ P ₀ ₄	Triplicate immersions in binder followed by autoclaving		Rabbit calvaria defects	Histomorphometry revealed that bone augmentation occurred within and over the 3D-printed block. ⁸³
Will, 2008	Binder jetting	CaP Powder: HA Binder: PEG-based binder	Sintered to 600, 1250 or 1400 °C		Rat subcutaneous implantation	Within 4 weeks of ectopic implantation, tissue ingrowth demonstrated fibrosis, granulocytic infiltration, and neovascularization ⁹²
Seol, 2014	Vat Polymerization	1 Urethane acrylate monomer (FA1260T) + HA 2 Urethane acrylate monomer (FA1260T) + TCP/HA	Sintered to 1400 °C	Human turbinate MSCs	Rat calvarial defect	TCP/HA scaffolds enhanced bone regeneration <i>in vivo</i> relative to HA scaffolds, and enhanced osteogenesis-related gene expression by MSCs <i>in vitro</i> compared to pure HA scaffolds ⁷²

HA hydroxyapatite, TCP tricalcium phosphate, oAEC ovine aorta endothelial cells, PCL poly(ϵ -caprolactone), OB osteoblasts, PDL periodontal ligament, PVA poly (vinyl alcohol), MSCs mesenchymal stem cells, VAM virus activated matrix, Ti titanium.

TABLE 6

Low-temperature 3D printing for drug delivery.

Reference	3D printing technology	Printed material(s)	Post-processing	Drug/growth factor	Cells/animal model	Primary findings
<i>In vitro</i> studies						
Akkineni, 2015	Material extrusion	CaP Paste (α -TCP + monetite (CaHPO ₄) + Calcium Carbonate (Ca- CO ₃) + HA in a liquid carrier of short-chain triglyceride	Setting by either submersion in water or in humidified air for 3 days followed by air drying at 37 °C	VEGF, BSA (Control)	hMSCs, hDMEC	Scaffolds cytocompatible with hMSCs, retained the biological activity of encapsulated VEGF ¹
Martinez-Vazquez, 2015	Material extrusion	Silicon-doped hydroxyapatite/gelatin slurry	Glutaraldehyde at 25 °C followed by air drying or lyophilizing	Vancomycin	MC3T3	Good cytocompatibility, first- order diffusive release with ~100% cumulative release in 10 h, inhibited bacterial growth ⁶⁴
Gbureck, 2008	Binder jetting	CaP Powder: TCP Binder: 10% H ₃ P ₀ ₄ + 0.5 M Ca(H ₂ P ₀ ₄) ₂	Triplicate 60 s immersions in binder with or without subsequent coating of PLGA	Vancomycin	N/A	Drug release was controlled for the ceramics matrices, whereas ceramics/polymer composites led to a mixed diffusion and degradation controlled release ⁶⁶
<i>In vivo</i> studies						
Poldervaart, 2013	Material Extrusion	Biphasic CaP (TCP + HA) granules in alginate hydrogel	Cross-linked in CaCl ₂	BMP-2 alone or in gelatin microparticles (GMPs) with gMSCs	SQ in mice or rats	Use of GMP carrier resulted in BMP-2 sustained release kinetics and bioactivity over three weeks leading to enhanced osteogenicity ⁷⁰
Barralet, 2009	Binder jetting	CaP Powder: α/β -TCP Binder: 20% H ₃ P ₀ ₄	Triplicate 60 s immersions in binder	Passive adsorption of VEGF, Copper Sulfate (CuSO ₄ as a source of Cu ²⁺)	Peritoneal cavity in mice	Low doses of Cu ²⁺ adsorption resulted in micro vessel growth <i>in vivo</i> which was enhanced in combination with VEGF ⁵

Reference	3D printing technology	Printed material(s)	Post-processing	Drug/growth factor	Cells/animal model	Primary findings
Gbureck, 2007	Binder jetting	CaP Powder: TTCP or TCP Binder: 10% H ₃ P ₀ ₄ + 1 M NaH ₂ P ₀ ₄ for TTCP and 20% H ₃ P ₀ ₄ for TCP	TTCP: binder then Na ₂ HPO ₃ dips TCP: Triplicate 60 s immersions in binder	Passive adsorption of VEGF, Copper Sulfate (CuSO ₄ as a source of Cu ²⁺)	Peritoneal cavity in mice	TCP scaffolds with either VEGF or copper sulfate had vascularized tissue in- growth. TTCP scaffolds had little tissue growth ³⁴
Inzana, 2015	Binder jetting	CaP Powder: α-TCP Binder: 8.75% H ₃ P ₀ ₄ + 0.25% Tween 80	Select scaffolds coated with PLGA	Vancomycin, Rifampin	Femoral OM defect in mice	Co-delivery of rifampin and vancomycin significantly improved outcomes of OM compared to the clinical standard of PMMA spacers. PLGA coating prolonged drug delivery and enhanced antimicrobial outcome ⁴⁴

CaP calcium phosphate, VEGF vascular endothelial growth factor, BSA bovine serum albumin, hMSCs human mesenchymal stem cells, HDMEC human dermal microvascular endothelial cells, TTCP tetracalcium phosphate, TCP tricalcium phosphate, HA hydroxyapatite, PLGA poly(lactic-co-glycolic acid), OM osteomyelitis, PMMA poly(methyl methacrylate).

TABLE 7

High-temperature 3D printing for drug delivery.

Reference	3D printing technology	Printed material(s)	Post-processing	Drug/growth factor	Cells/animal model	Primary findings
<i>In vitro</i> studies						
Duan, 2010	Powder bed fusion	CaP/PHBV microspheres	Physical entrapment of gelatin and heparin immobilization, followed by binding of BMP-2 to the surface or simple BMP-2 adsorption	BMP-2	SaOS-2 and C3H10T1/2 cells	Surface modification improved binding affinity to BMP-2 as demonstrated by the enhanced cytocompatibility of seeded C3H10T1/2, and upregulation of ALP activity and osteogenic gene expression ²³
Gbureck, 2007	Binder jetting	CaP Powder: TTCP or TCP Binder: 10% H ₃ PO ₄ + 0.5 M Ca(H ₂ PO ₄) ₂ for TTCP and 10% H ₃ PO ₄ + 0.5 M Ca(H ₂ PO ₄) ₂ for TCP	TTCP: heated to 150°C for 1 h, dip in binder, boil for 2 h in 2.5% Na ₂ HPO ₄ TCP: dip in binder Select scaffolds also impregnated with PLGA	Vancomycin, ofloxacin, and tetracycline <i>via</i> passive adsorption or vacuum loading		Adsorption and desorption kinetics were primarily based on physical characteristics (i.e., specific surface area) rather than chemical composition. The addition of a polymer component enabled a controlled release profile depending on molecular size ³⁷
<i>In vivo</i> studies						
Ishack, 2015	Material extrusion	β -TCP + HA particles in colloidal gel ink	Sintered in steps in the range of 400–1100°C, followed by surface coating with collagen	Dipyridamole, BMP-2	Mouse cranial defect	Dipyridamole and BMP-2 loaded scaffolds demonstrated significant bone formation and bone remodeling compared to a drug free scaffolds. Specificity of Dipyridamole was confirmed by lack of effect in A2AKO mice ⁴⁵
El-Ghannam, 2007	Binder jetting	CaP Powder: CaP + silica Binder: sugar-based binder	Sintered in steps between 450 and 900°C	BMP-2	Rabbit ulna defect	Scaffolds provided a sustained release of BMP-2 at an effective dose for up to 14 days <i>in vitro</i> , and enhanced torsional strength of healed ulnas compared to control ²⁶
El-Ghannam, 2013	Binder jetting	CaP Powder: CaP + silica Binder: sugar-based binder	Sintered in steps between 450 and 900°C	BMP-2	Rabbit ulna defect	Porosity characteristics needed for bioactivity were maintained after sintering. No signs of toxicity <i>in vivo</i> ; new bone formation and cell-mediated resorption and dissolution of the scaffold were observed ²⁷
Strobel, 2014	Binder jetting	CaP Powder: β -TCP + HA + potato starch powder (dextrin) Binder: Water-glycerol	Stepwise heating 75–350°C then sintering at 1200°C, followed by coating with fibrin (TISSEEL)	BMP-2, and/or Primary OB cells	SQ in rats	Adding OB and BMP-2 to scaffolds synergistically enhanced ectopic bone formation ⁷⁸

Author Manuscript

Author Manuscript

Author Manuscript

Author Manuscript

PHBV poly(hydroxybutyrate-co-hydroxyvalerate), *CaP* calcium phosphate, *BMP-2* bone morphogenetic protein 2, *ALP* alkaline phosphatase, *TTCP* tetracalcium phosphate, *7TCP* tricalcium phosphate, *HA* hydroxyapatite, *PLGA* poly(lactic-co-glycolic acid), *SQ* subcutaneous, *OB* osteoblasts.